Kovove Mater. 51 2013 1–10
DOI: 10.4149/km_2013_1_1

Cr_xN_y coatings prepared by magnetron sputtering method

M. Béger[1], P. Jurči[1]*, P. Grgač[1], S. Mečiar[1], M. Kusý[1], J. Horník[2]

[1] *STU, MtF in Trnava, J. Bottu 52, SK-917 24 Trnava, Slovak Republic*
[2] *CTU in Prague, Faculty of Mechanical Engineering, Karlovo nám. 13, CZ-121 35 Prague, Czech Republic*

Received 17 July 2012, received in revised form 24 October 2012, accepted 7 November 2012

Abstract

Chromium nitride coatings were deposited by reactive magnetron sputtering onto substrates made from Cr-ledeburitic steel 1.2379. Microstructures, phase constitution, mechanical and tribological properties of CrN-coatings were investigated. It has been found that the deposition at given combination of parameters gave dense, fine-grained coatings, having columnar structure and very smooth surface. The coatings were formed from Cr_2N when low N_2 : Ar ratio has been used while they contained CrN at higher nitrogen input into the processing chamber. The Young's modulus of the coatings was influenced only slightly by the deposition conditions. On the other hand, the hardness of the CrN was higher than that of the Cr_2N. The adhesion of the CrN is better than that of Cr_2N. The principal explanation is that the Cr_2N is brittle in nature and exhibits a strong tendency to cracking and spallation when normally loaded. Generally, the friction coefficient measured against 100Cr6 ball bearing steel was lower than that determined against sintered alumina. Considerable material transfer (adhesion) has been recorded for 100Cr6-steel while no transfer but abrasion has been detected for alumina counterpart. For the alumina counterpart, better tribological behavior has been recorded for the CrN than that for Cr_2N, which is consistent with its good adhesion.

K e y w o r d s: ledeburitic steel substrate, magnetron sputtering, CrN-coating, microstructure, mechanical properties, tribology

1. Introduction

Chromium nitride (Cr_xN_y) hard coatings have been developed over the past two decades. They have early gained a great scientific interest due to their good wear- and corrosion resistance, up to very high temperatures [1–3]. The chromium nitride coatings are used in a variety of applications such as tools for wood machining [4, 5], cutlery industry [6], ultra-high speed micro-machining [7], automotive industry [8], and biomedicine [9]. Another important field of their application is the nuclear industry as hard facing material due to their excellent anti-galling properties and high thermal stability [10]. Besides that, it is possible to deposit fine-grained CrN-films up to a relatively great thickness (around 7 μm) whereas low internal stresses are kept. This fact together with that CrN is less brittle than TiN, but still quite hard, makes CrN more suitable for surface protection at relatively soft substrates such as aluminum alloys and stainless steels [3].

The Cr_xN_y coatings are generally manufactured by various physical vapor deposition (PVD) methods such as the arc deposition and reactive magnetron sputtering [13]. Magnetron sputtering has been developed rapidly over the last decade. This deposition technique offers the same or better functionality of the films than the others, but at greater film thickness. It now makes a significant impact in application areas including hard, wear-resistant coatings, low friction coatings, corrosion-resistant coatings, and decorative coatings [11].

The effect of the nitrogen partial pressure on the phase constitution of magnetron sputtered chromium nitride coatings has been studied extensively [2, 12–15]. It has been established that the phase constitution of the coatings was changed from the Cr(N) solid solution at very low nitrogen partial pressure to the mixtures of Cr(N) + Cr_2N or Cr_2N + CrN when higher nitrogen partial pressure has been used. At specific conditions, pure either Cr_2N or CrN were obtained.

The opinions on the effect of the nitrogen partial

*Corresponding author: e-mail address: p.jurci@seznam.cz

Table 1. Deposition variables of the processes

Samples	Processing variables	
	Substrate bias (V)	Reactive atmosphere $N_2 : Ar$ ($cm^3\ min^{-1}$)
4, 5, 6	–100	30 : 90
7, 8, 9	–100	60 : 60
10, 11, 12	–75	20 : 90
13, 14, 15	–75	30 : 90
16, 17, 18	–75	60 : 60
19, 20, 21	–50	20 : 90

pressure on the grain size of the coatings are adverse. Shah et al. [12] have established a refinement in the grain size scale with increased nitrogen partial pressure while Logothetidis et al. [17] have reported an opposite tendency. In addition, the density of the films is closely related to the nitrogen partial pressure. Here, a good agreement on this effect can be found in the literature – the higher nitrogen partial pressure the denser are the coatings [12, 19]. The film with the maximal density can be produced by reactive HIPIMS technique [18]. Moreover, the application of this technique led to a very smooth coated surface, without droplets or other macroscopic growth defects.

The chromium nitride coatings grow mostly in a columnar manner [13, 18, 19] but the columnar character of the film growth can be changed to the granular mode when extremely high negative substrate bias is used for the film manufacturing [14].

Generally, the hardness of the chromium nitride thin films is higher when they contain Cr_2N-phase [12–14, 16, 20] than those formed of CrN. However, some other authors reported also rather opposite tendency or they established the same hardness for both phases [5]. The lower hardness values for CrN compared with those of Cr_2N films, which were established in the dominant part of the investigations, were attributed to higher degree of bond ionicity in the CrN phase. The Young's modulus of the chromium nitride films was higher also for the Cr_2N [13].

The chromium nitride films contain high compressive residual stresses [19]. These stresses can be responsible for lower adhesion of the films and their early damage. For this reason, Odén [21] and Broszeit [22] independently suggested the heat treatment (annealing) to modify the stress situation. After the application of proper heat treatment, the residual stresses were lowered to 30 % compared to those as deposited [21, 22].

Adhesion of the films onto the substrate is a critical point, which determines their suitability for an industrial use. It has been established recently that the CrN coating had a higher adhesion (being represented by the critical load determined by scratch test) than the Cr_2N coating of the same thickness [19]. Very good adhesion of the Cr_xN_y films can be achieved by using of the HIPIMS technique for their manufacturing [18]. Both the wear resistance and the friction coefficient of the films depend on their phase constitution. The wear resistance of the films containing the CrN is better than that of Cr_2N [16]. In the case of the films formed of the Cr_2N, increasing negative bias voltage led to a better wear resistance [14]. In addition, the friction coefficient against alumina counterpart was found to be lower for CrN [13].

The main goal of the current paper is to make serious investigations of the chromium nitride films produced at one of newest PVD devices, using a UB magnetron sputtering and for wide range of processing parameters.

2. Experimental

2.1. Coating deposition

Chromium nitride coatings were deposited on flat specimens ($15 \times 32 \times 12\,mm^3$) made from the AISI D2 (DIN 1.2379) with a nominal chemical composition (in wt.%): 1.6 % C, 12 % Cr, 0.7 % Mo, 1 % V, and Fe as a balance. The samples were austenitized in the vacuum furnace at a temperature of 1050 °C with the hold of 30 min, nitrogen gas quenched and twice tempered at 500 °C for 2 h. After that, the samples were mechanically polished using a diamond suspension (grain size up to 0.7 μm) to a mirror finish. The deposition has been carried out using magnetron-sputtering device Hauzer Flexicoat 850 at various combinations of processing parameters. The substrate temperature was kept in a narrow range between 250 and 260 °C. Two chromium targets with 99.98 % purity, opposite positioned, were used. The cathode output power has been kept at 2.9 kW on each cathode (target) during the deposition. The processing variables were the negative substrate bias (–50, –75 and –100 V) and the composition of the reactive atmosphere being represented by the ratio of N_2 and Ar, respectively. The combinations of processing variables are shown in Table 1. Three samples were treated at

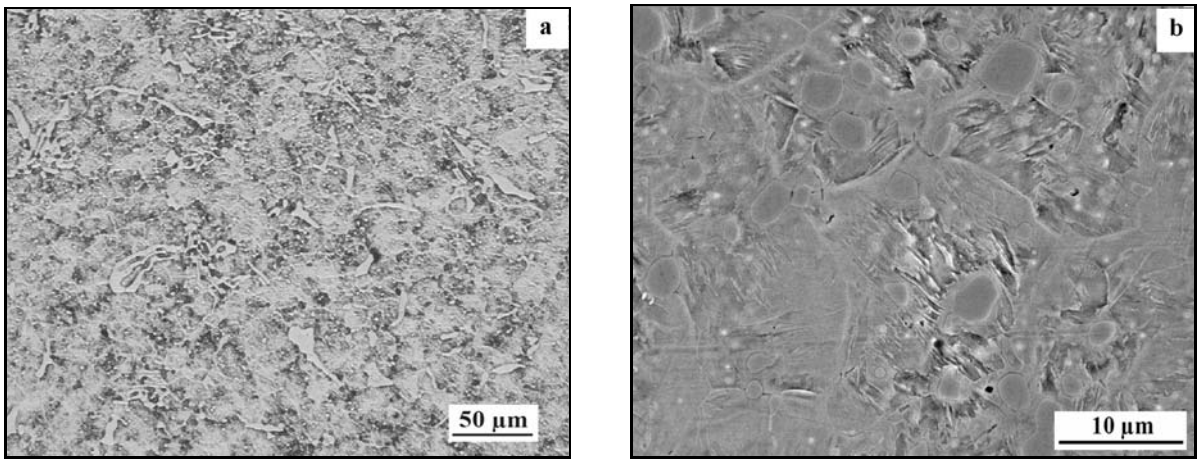

Fig. 1. Microstructure of as-heat treated substrate material: a) light micrograph, b) SEM micrograph.

any combination of processing variables.

Prior to deposition, all the samples were ultrasonically cleaned in an acetone, dried and fixed onto a rotating holder. The holder was then inserted into the processing chamber. Just prior to deposition, the samples were sputter cleaned in a pure argon atmosphere for 20 min. The rotation speed was adjusted to 2 rpm. The total deposition time was 6 h in all the cases.

2.2. Coating characterization

The microstructure of the substrate material has been investigated using the microscopy and scanning electron microscopy (SEM). For the coatings investigation, the SEM has been used only. The acceleration voltage was standard 15 kV.

The thickness of the films has been determined by the measurements on fracture surfaces of coated samples. Ten measurements of the thickness were made on each specimen and the average value was then calculated. Surface roughness was measured by laser confocal microscope Zeiss LSM 700.

Adhesion of the coatings has been measured by Revetest scratch tester. Standard Rockwell diamond indenter with a tip radius of 0.2 µm has been used. The initial loading was 1 N and it increased progressively to 100 N, at a rate of 49.5 N min^{-1}. Five measurements have been done on each specimen. The adhesion was evaluated as from the acoustic emission records so from the viewing of the scratches. The first symptoms of the flaking of the coating were chosen as a criterion for the determination of critical load.

The friction coefficient has been determined by the Pin-On-Disc method. The balls with a diameter of 6 mm, made from 100Cr6 ball bearing steel (hardness of 735 HV) and sintered alumina (Al_2O_3), were used as counterparts. The total sliding distance was chosen to be 100 m. No external lubrication has been used. The tests were performed at ambient temperature and relative humidity of 60 %.

The nanohardness and the Young's modulus (E) of the films have been measured using TTX NHT nanohardness tester (CSM Instruments). The so-called "linear mode" has been used, e.g. the loading increased progressively from the zero up to the maximum value of 200 mN. The loading time was 1 min and the hold at the maximal load was 20 s. Standard Berkovich nanoindenter has been used for the indentation. Ten measurements were done on each specimen, and the mean value and the standard deviation were calculated, respectively.

X-ray diffraction analysis has been used for the identification of phases in the coatings. The Phillips PW 1710 diffractometer with Fe filtered $Co_{K\alpha 1,2}$ characteristic radiation, in a Bragg-Brentano arrangement has been employed. Data were recorded in the range 30–140° of the two-theta diffraction angle.

3. Results and discussion

3.1. Substrate characterization

The microstructure after performed heat treatment is shown in Fig. 1. Light micrograph, Fig. 1a, demonstrates that the material is composed of the matrix and undissolved carbides. Detail SEM micrograph, Fig. 1b, shows that the matrix is formed by needle-like tempered martensite. The carbides are mainly of the M_7C_3 nature, as previously reported [27]. The final as-tempered hardness of the samples was 61 HRC.

3.2. Microstructure of the films

SEM micrographs, Fig. 2, show how the coatings have grown at different deposition conditions. All the

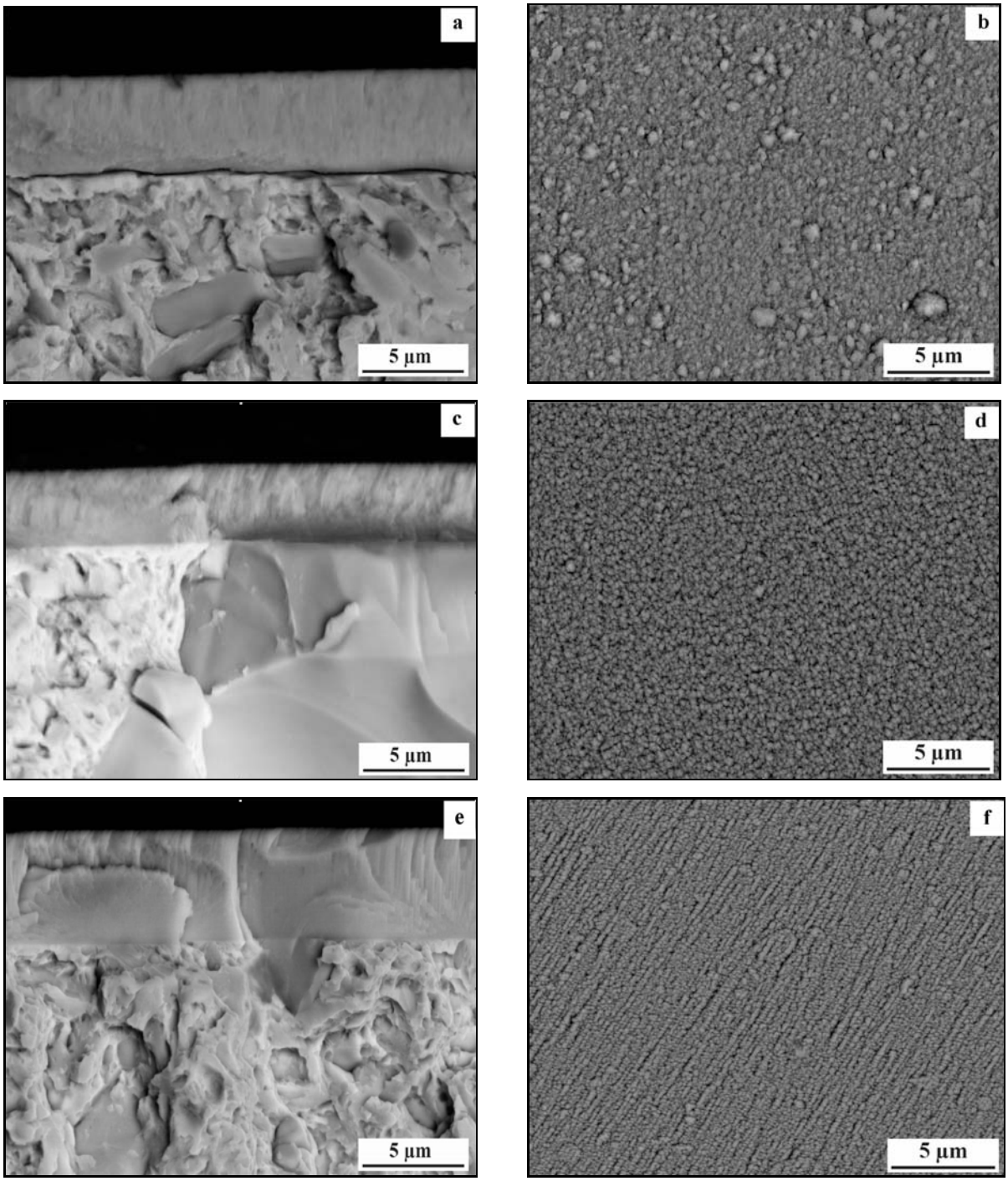

Fig. 2a–f. Cross-sectional and plane view SEM images of Cr_xN_y coatings deposited on DIN 1.2379 substrate: a), b) Sample 4, bias of –100 V, N_2 : Ar = 30/90; c), d) Sample 7, bias of –100 V, N_2 : Ar = 60 : 60; e), f) Sample 10, bias of –75 V, N_2 : Ar = 20/90.

coatings have dense structure, without any inhomogeneities like pores or cracks. The coating/substrate interface is also free of defects in almost all the cases. Only in the case of the coating formed at a bias of –100 V, N_2/Ar = 30/90, the cohesive failure on the interface can be seen, Fig. 2a. The thickness of the film was 4.1 µm. The film grew in a typical columnar manner, with well visible individual crystals. Plan-view micrograph, Fig. 2b, shows that the surface exhibits non-uniform structure, combined of two types of features. The first type of feature is the semi-equiaxial grains (SEG) with a size of 0.2–0.5 µm. This feature makes dominant area portion of the surface and can be called as a "matrix". In this "matrix", several form-

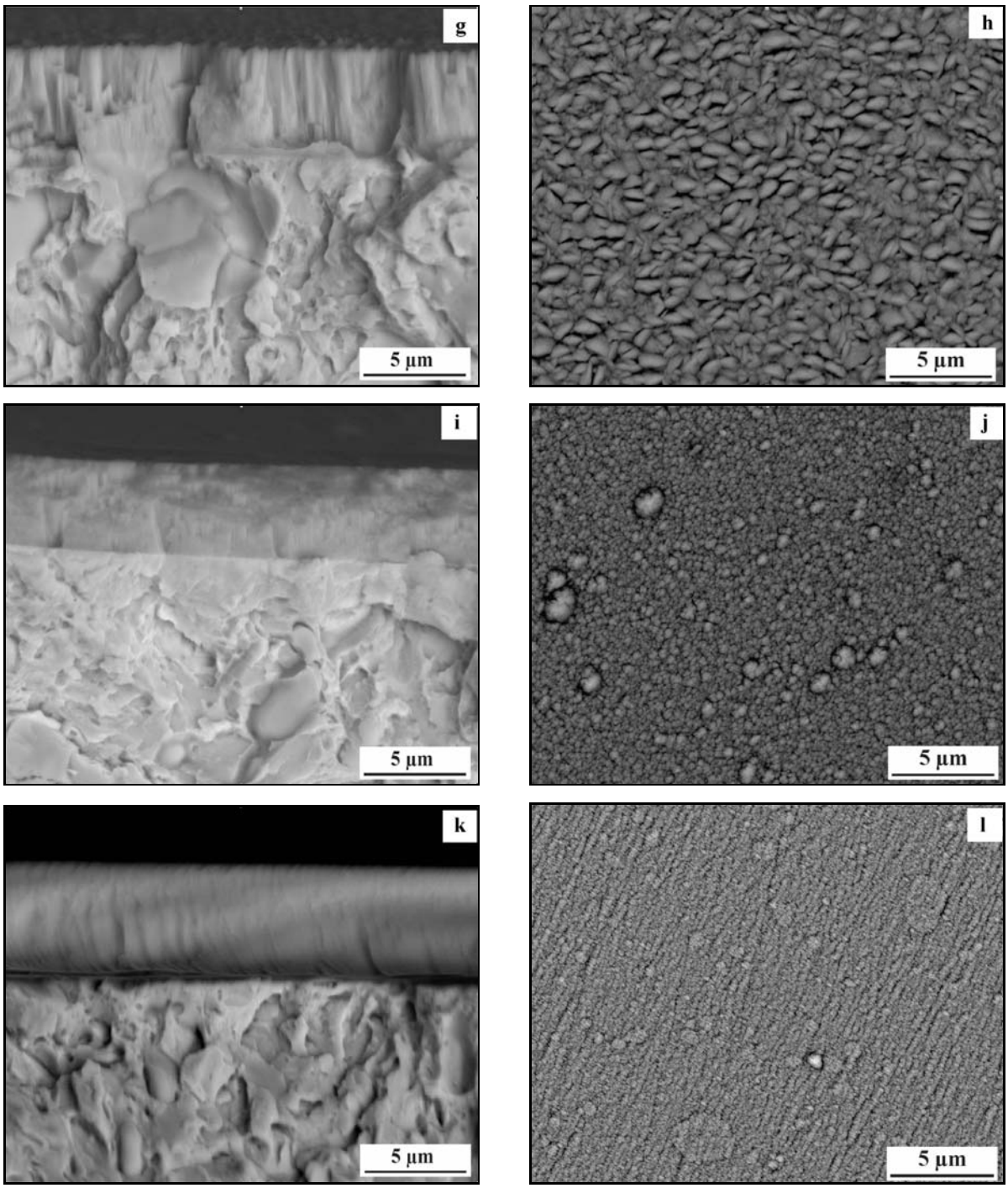

Fig. 2g–l. Cross-sectional and plane view SEM images of Cr_xN_y coatings deposited on DIN 1.2379 substrate: g), h) Sample 13, bias of –75 V, $N_2 : Ar = 30 : 90$; i), j) Sample 16, bias of –75 V, $N_2 : Ar = 60/60$; k), l) Sample 21, bias of –50 V, $N_2 : Ar = 20 : 90$.

ations that can be described as cauliflower-like (CFL) structure are embedded. Similar surface structure of chromium nitride films has been already reported and discussed by Zhao et al. [28]. They established that the combination of "equiaxially grained" (or facetted) and cauliflower-like structures is typical for two-phased (CrN and Cr_2N) films. However, no two phases were identified in the given coating by X-ray diffraction. One can thus assume that: i) the combination of above described microstructural formations can not always be attributed to the presence of two chromium nitrides in the coating or ii) the coating is two-phased but the amount of CrN is below the detection limit of the used experimental technique.

The thickness of the film produced at a bias of –100 V and $N_2 : Ar = 60 : 60$ was 3.3 µm, Fig. 2c. In

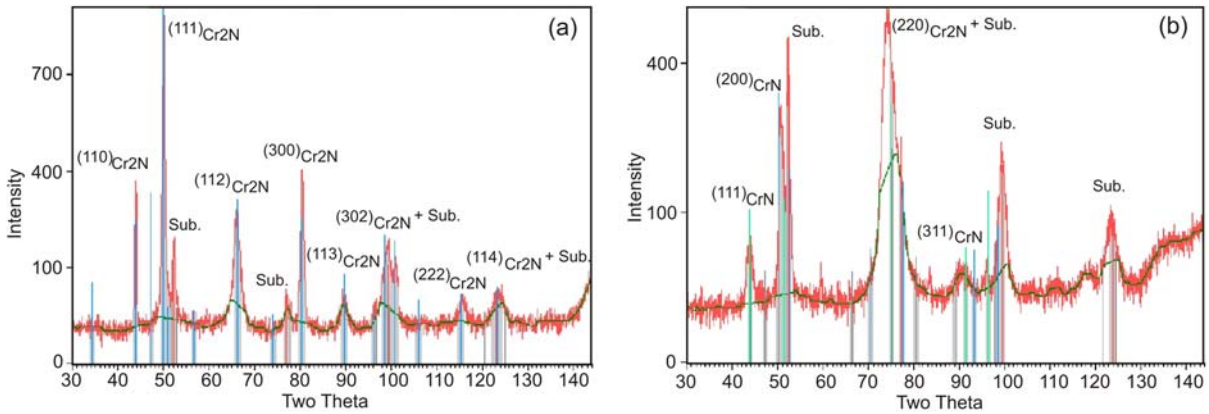

Fig. 3. X-ray diffraction patterns of the coatings produced at: a) bias of –75 V and $N_2/Ar = 30:90$, b) bias of –75 V and $N_2 : Ar = 60:60$.

a similar way to the previous case, the film grew in a columnar manner. Individual crystals are visible, also. Plan-view SEM micrograph, Fig. 2d, demonstrates that no cauliflower-like formations are presented in the surface microstructure of the film and the film is composed of semi-equiaxial grains (visible on the plan-view picture) only. Moreover, the grains are refined compared to the film produced at lower nitrogen content in the reactive atmosphere.

Figure 2e demonstrates that the thickness of the film was 4.9 μm when an atmosphere with $N_2 : Ar = 20:90$, at a bias of –75 V, was applied. Individual columnar crystals are also well visible. The surface structure is very fine with practically no presence of coarse grains on the surface, Fig. 2f. Compared to the film grown at a bias of –100 V and $N_2 : Ar = 30:90$, the application of a bias of –75 V at the same ratio of atmosphere components led to slightly greater thickness of the films, Fig. 2g. The thickness of the film was 4.3 μm. Sharp-edged crystals of the Cr_2N are visible on the fracture surface. Plane-view SEM micrograph in Fig. 2h demonstrates a coarsening of the microstructure compared to the film produced at lower N_2 content whereas the rice-like formations are the dominant feature of the coating. An increase in nitrogen content to $N_2 : Ar = 60:60$ gave thinner film (thickness of 3.9 μm) and the crystals became practically invisible on the fracture surface, Fig. 2i. On the plane-view micrograph, Fig. 2j, there is a large microstructural inhomogeneity apparently shown. The microstructure consists of two basic types of features. The first one is the "matrix" formed by semi-equiaxial grains of a size ranging between 0.3 and 0.5 μm, and the second type of the feature are the cauliflower-like formations as described above, Fig. 2b.

The deposition carried out at a bias of –50 V and $N_2 : Ar = 20:90$ gave the highest thickness of the film, Fig. 2k. The total film thickness was measured to be 5.3 μm. The structure of the film contains well visible individual crystals with no sharp topography on the fracture surface. Plan-view SEM micrograph, Fig. 2l, shows that the structure of the coating is quite inhomogeneous and contains two features, in a similar way to the films produced at a bias of –75 V in the atmosphere with $N_2 : Ar = 60:60$.

The measurements of surface roughness did not give doubtless results. Moreover, the surface roughness remained very low after the film deposition and it ranged between 7 and 22 nm, excepting a few cases where micro-particles were recorded on the surface. It can be assumed that no relevant effect of the roughness on film properties can thus be expected. Similar expectations were also suggested by Lin et al. [23] for UB magnetron sputtered semi-stoichiometric CrN films deposited onto stainless steel substrate.

3.3. Phase constitution

X-ray diffraction revealed that the coatings created in reactive atmospheres containing $N_2 : Ar$ of 20 : 90 and 30 : 90, respectively, are formed from the Cr_2N while those grown in the atmosphere with $N_2 : Ar = 60:60$ are of the CrN, as shown in Fig. 3a,b, and summarized in Table 2. This seems to be logical because CrN contains more N than Cr_2N, and higher nitrogen amount in the reactive atmosphere should promote growth of the phase with higher N content. Moreover, the mentioned observation is consistent with other findings reported previously [1]. In addition, it should be noticed that the data obtained by the X-ray diffraction do not represent only the surface phase constitution but, due to the penetration of the X-rays, the X-ray patterns also represent the phase constitution of the substrate.

3.4. Friction coefficient

Generally, the measurements of the friction coefficient μ gave lower values when the balls made from 100Cr6 steel were used as counterparts, Table 2. The

Table 2. Phase constitution, mechanical properties, friction coefficient μ and critical loads of developed chromium nitride coatings

Deposition bias, $N_2 : Ar$	–100, 30/90	–100, 60/60	–75, 20/90	–75, 30/90	–75, 60/60	–50, 20/90
Major phase	Cr_2N	CrN	Cr_2N	Cr_2N	CrN	Cr_2N
Nanohardness (GPa)	21.8 ± 1.25	25 ± 3	23.1 ± 1.5	17.3 ± 2.8	23.1 ± 3.9	20 ± 5
E (GPa)	225 ± 12.5	240 ± 20	224 ± 7	216 ± 37.3	212 ± 38.5	223 ± 9.5
μ-100Cr6	0.28	0.29	0.27	0.24	0.23	0.36
μ-Al_2O_3	0.59	0.40	0.65	0.72	0.39	0.68
Critical load (N)	31	56.3	46.4	63	56.6	41

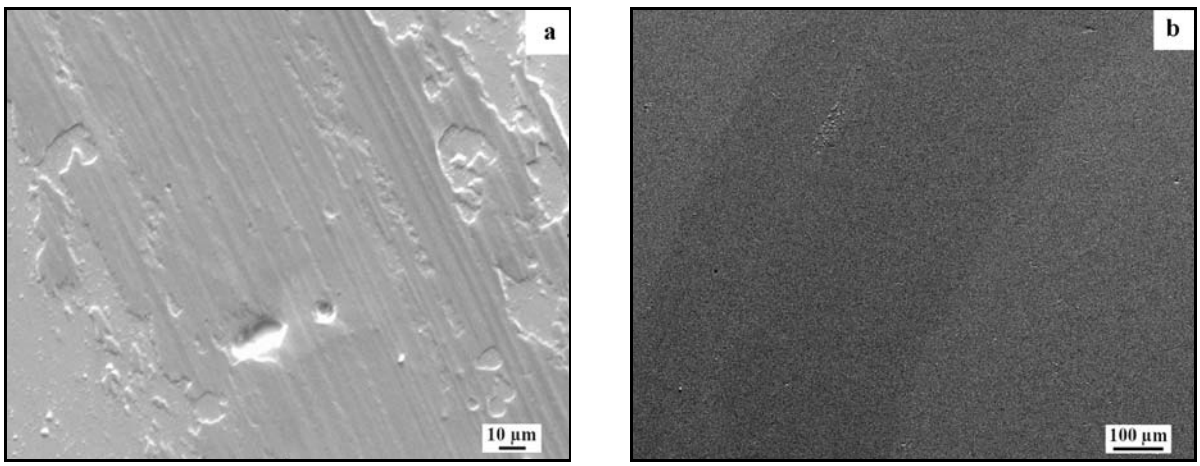

Fig. 4. SEM micrographs of wear scares resulted from the sliding of 100Cr6-steel ball on the surface: a) the CrN film grown at –75 V and $N_2 : Ar = 60 : 60$, b) the Cr_2N film grown at –50 V and $N_2 : Ar = 20 : 90$.

μ ranged between 0.23 and 0.36 whereas lower values were recorded for the coatings made at a bias voltage of –75 V and the highest friction coefficient had the film produced at a bias of –50 V. For the alumina counterpart, the average friction coefficient ranged in very wide range from 0.39 to 0.72. The actual value of the μ depended on the nature of the film, e.g. the μ was detected to be lower for the pure CrN while it was considerably higher for the Cr_2N.

The differences between the friction coefficients recorded on various samples can be explained as follows:

a) 100Cr6 steel used as a counterpart – Figure 4 brings top view micrographs of the wear scares obtained by the sliding of the counterpart on the surface of the films produced at –75 V and $N_2 : Ar = 60 : 60$ and –50 V and $N_2 : Ar = 20 : 90$, respectively. The first wear scare is almost completely covered with transferred material from the counterpart, while the second scare is almost free of any adhered material. Thus, no friction coefficient of the sliding couple film/100Cr6--steel but that of 100Cr6/100Cr6 has been rather recorded in the first case. In the second case, real μ from the sliding couple Cr_2N-film/100Cr6-steel has been measured. It is worth noticing that no effect of the dominant phase on the friction coefficient has been established – mainly due to the fact that the transfer of the counterpart's material occurred even during early stage of the sliding (running up stage) and no real friction coefficient could have been recorded further (steady stage). These results are, however, inconsistent with other investigations, e.g. [24]. In this paper, the testing of magnetron sputtered Cr_xN_y-films against GCr15 steel (hardness of 610 HV) gave much lower friction coefficient for Cr_2N than that for CrN. Unfortunately, it is not clear from the paper what happened at the film/counterpart interface during the tests, and therefore it is hard to explain the nature of different wear behavior of investigated sliding couple in our trials.

b) Alumina used as a counterpart – It is clearly shown that the films formed by CrN had much lower friction coefficient than those formed by Cr_2N. Figure 5 shows top view SEM micrographs of two samples with completely different wear behavior. The wear scare of the film formed at a negative substrate bias of 100 V and $N_2 : Ar = 60 : 60$ had a very smooth surface with no symptoms of particles removal during the tests, Fig. 5a. The wear scare of the sample layered at a bias of –75 V and $N_2 : Ar = 30 : 90$, Fig. 5b, contains a lot of craters and places with complete removal of the film. Removed particles (wear debris) also yield to elevated abrasion and thereby to higher friction coef-

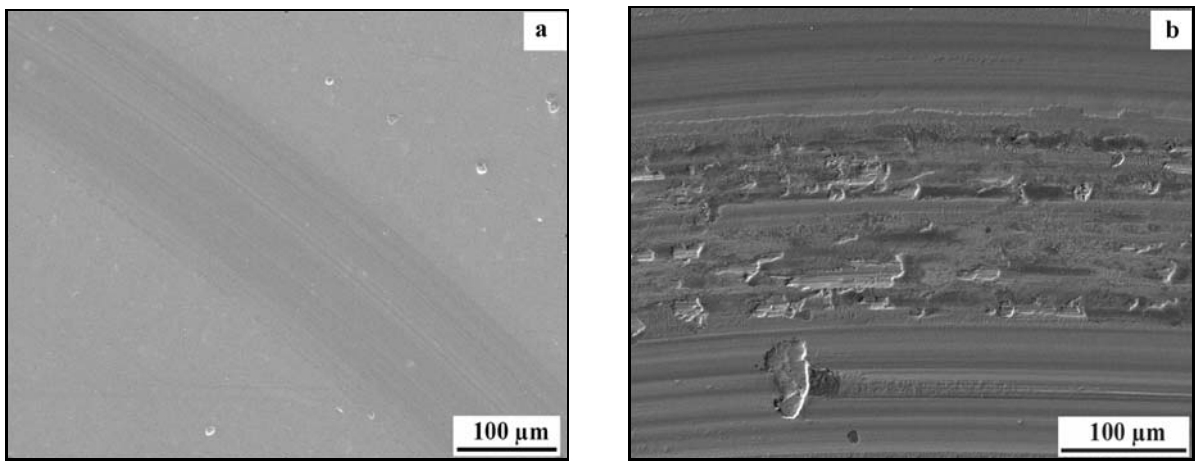

Fig. 5. SEM micrographs of wear scares resulted from the sliding of alumina ball on the surface: a) the CrN film grown at –100 V and $N_2 : Ar = 60 : 60$, b) the Cr_2N film grown at –75 V and $N_2 : Ar = 30 : 90$.

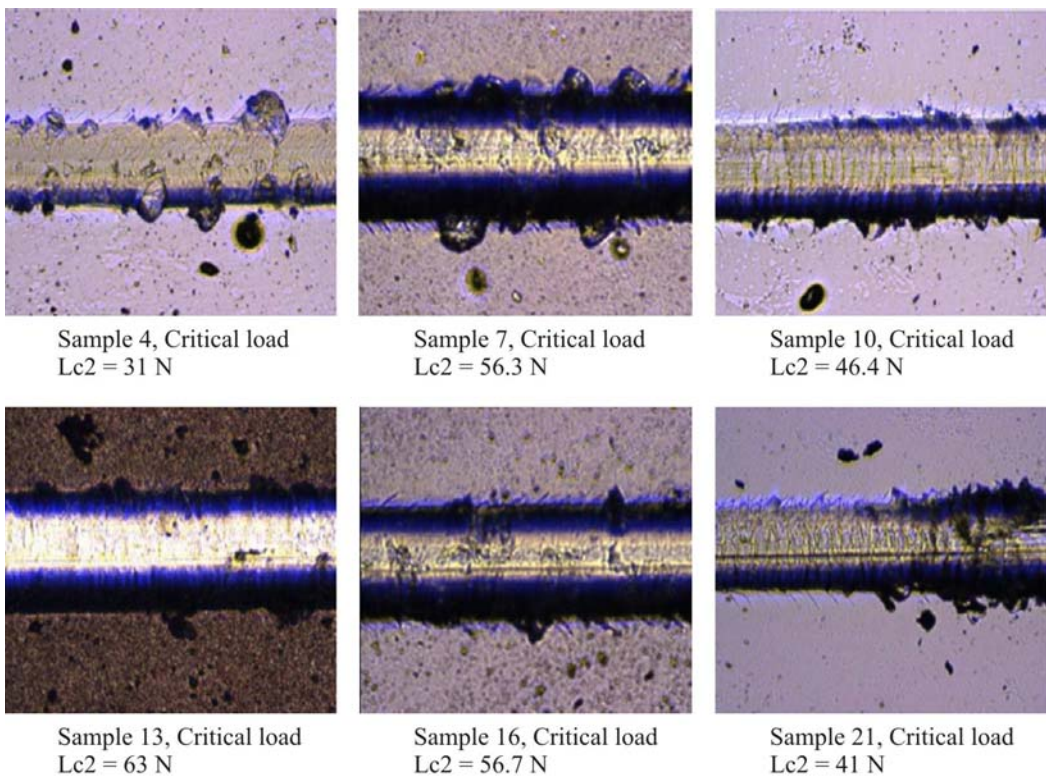

Fig. 6. Light micrographs showing the scratches made on investigated Cr_xN_y films.

ficient. It should be noted that the Cr_2N is rather slightly softer than the CrN, Table 2, although many experiments fixed an opposite tendency [4, 8, 15, 19, 26] or established similar hardness for both phases [5]. Moreover, the Young's modulus of both phases was recorded to be different only in a very limited extent. The consideration that the differences between the substrate properties (hardness, Young's modulus) and the same properties of the films are a criterion for the adhesion [29] has a limited validity here. Possible logical interpretation of obtained results could be given using the Hurkmans's findings. In his early study he established that lower critical load of the Cr_2N is systematic due to the brittleness nature of the hexagonal Cr_2N compared to cubic CrN [32].

3.5. Adhesion

The results of the adhesion measurements are summarized in Table 2. It is worth noticing that the critical load rather increases with the increase of nitrogen portion in the reactive atmosphere. However, there is

an exception in this "general tendency" – the best adhesion was found for the film formed at $N_2 : Ar = 30 : 90$ when a bias of –75 V has been applied. The difference, compared to the film made at $N_2 : Ar = 60 : 60$, is relatively small. Nevertheless, the general statement that the CrN has better adhesion than the Cr_2N is not valid in this case, and this finding is rather inconsistent with other observations [4, 26, 32] where slightly higher adhesion of CrN was recorded. Other investigations [25] revealed a direct dependence of the adhesion values on the nanohardness of the coatings. However, there is no data on the phase constitution of investigated thin films given, which makes it impossible to decide on the effect of phase constitution on the film adhesion.

During the scratch-test, the failure of the coatings begins with either semi-circular tensile cracking or with side-flaking, Fig. 6. There can not be a direct dependence between the failure manner (critical load) and the coating preparation route established. For example, the failure of the Cr_2N coating prepared at a bias of –100 V and $N_2 : Ar = 30 : 90$, began with the side-flaking on both sides of the scratch, Fig. 6. The critical load for this film was 31 N. The same mechanism, however, has been determined for the failure initiation in the case of the Cr_2N film grown at a bias of –75 V and $N_2 : Ar = 30 : 90$. Nevertheless, this film had the best adhesion and the critical load was 63 N. These results are well consistent with the microstructural analysis, see Fig. 2. Cross-sectional SEM micrograph of the Cr_2N film prepared at a bias of –100 V and $N_2 : Ar = 30 : 90$ indicated symptoms of cohesive failure, which was confirmed via the scratch test (the lowest value of the critical load). In other cases of the films, no inhomogeneities at the film/substrate interface were found, which is consistent with the adhesion measurements. Anyway, it seems that further amelioration of adhesion of pure Cr_xN_y thin films has some limitations. One of possible ways how to achieve higher adhesion is the deposition of either nano-structured films with incorporated soft phases [30] or duplex coatings [31]. Investigations of mentioned coatings types allow to suggest that the coatings can store a higher amount of plastic deformation energy (work of fracture) preceding the failure, which results in higher adhesion onto the ledeburitic steel substrates.

Table 2 summarizes the results of nanohardness measurements and the determination of the Young's modulus of the films. The nanohardness of the CrN films was recorded to be slightly higher than that of Cr_2N. The average values of the Young's modulus ranged between 212 and 240 GPa, independently on the fact whether the film was formed with CrN of Cr_2N. Moreover, the values exhibited large scatter and overlap. One can thus say that the Young's modulus is either practically unaffected or is influenced only negligibly by the deposition parameters within their range investigated.

The first finding seems to be rather unexpected. Many authors have reported an opposite tendency, e.g. the Cr_2N has slightly higher hardness than the CrN [4, 8, 15, 19, 26]. Other authors, for instance Nouveau at al. [5] arrived to finding that the hardness of both phases is similar. It should be noticed, however, that: 1. In most cases of investigations, no ledeburitic steels were used as substrates for the film deposition and the formation of the films was influenced by the nature of the substrates; 2. In above mentioned papers, different deposition techniques at completely different combinations of processing parameters were used, which makes the direct comparison of obtained results difficult or almost impossible.

4. Conclusions

The results of the investigation of magnetron sputtered Cr_xN_y thin films on the DIN 1.2379 ledeburitic steel substrate arrived to the following findings:

The thickness of the films increased with decreased negative substrate bias. At a constant substrate bias, increased nitrogen input led to lowered film thickness.

All the coatings exhibited dense structure, without any inhomogeneities.

The films grew in a typical columnar manner. After the deposition, the coated surfaces were very smooth, with only minimal number of micro-particles.

The films formed in low-nitrogen containing atmospheres consisted of Cr_2N-phase while those grown in the atmosphere with $N_2 : Ar = 60 : 60$ contained CrN--phase.

The nanohardness of CrN was, rather unexpectedly, slightly higher than that of Cr_2N. The Young's modulus of both compounds was found to be influenced by the processing parameters only in a very limited extent.

The friction coefficient was lower for the 100Cr6 steel counterpart than that for alumina. For the 100Cr6 counterpart, material transfer from the ball to the sample has been recorded, which made the results hardly comparable. The lowest friction coefficient, when alumina ball has been used, was determined for CrN. This is because the Cr_2N underwent cracking and delamination during the testing, formed wear debris, which contributed to the increase of the μ.

The results on the friction coefficient are consistent with the adhesion determination – the better adhesion the lower is the friction coefficient against alumina.

Acknowledgements

This paper is a result of the project implementation: Center for the development and application of advanced

diagnostic methods in processing of metallic and non-metallic materials, ITMS:26220120048, supported by the Research & Development Operational Programme funded by the ERDF. Further, authors wish to thank F. Lofaj for providing measurements of mechanical characteristics of the coatings.

References

[1] Frederick, J. R., D'Arcy-Gall, J., Gall, D.: Thin Solid Films, *497*, 2006, p. 330. doi:10.1016/j.tsf.2005.08.244
[2] Nam, K. H., Jung, M. J., Han, J. G.: Surface and Coatings Technology, *131*, 2000, p. 222. doi:10.1016/S0257-8972(00)00813-6
[3] Elangovan, T., Kuppusami, P., Thirumurugesan, R., Ganesan, V., Mohandas, E., Mangalaraj, D.: Materials Science and Engineering, *B167*, 2010, p. 17. doi:10.1016/j.mseb.2010.01.021
[4] Djouadi, M. A., Nouveau, C., Beer, P., Lambertin, M.: Surface and Coatings Technology, *133–134*, 2000, p. 478. doi:10.1016/S0257-8972(00)00980-4
[5] Nouveau, C., Jorand, E., Decés-Petit, C., Labidi, C., Djouadi, M.-A.: Wear, *258*, 2005, p. 157. doi:10.1016/j.wear.2004.09.034
[6] Hovsepian, P. Eh., Münz, W.-D., Medlock, A., Gregory, G.: Surface and Coatings Technology, *133–134*, 2000, p. 508. doi:10.1016/S0257-8972(00)00921-X
[7] Shin, S. H., Kim, M. W., Kang, M. C., Kim, K. H., Kwon, D. H., Kim, J. S.: Surface and Coating Technology, *202*, 2008, p. 5613. doi:10.1016/j.surfcoat.2008.06.128
[8] Wei, R., Langa, E., Rincon, C., Arps, J. H.: Surface and Coatings Technology, *201*, 2006, p. 4453. doi:10.1016/j.surfcoat.2006.08.091
[9] Wei, G., Rar, A., Barnard, J. A.: Thin Solid Films, *398–399*, 2001, p. 460. doi:10.1016/S0040-6090(01)01388-8
[10] Kuppusami, P., Dasgupta, A., Raghunathan, V. S.: ISIJ Int., *42*, 2002, p. 1457. doi:10.2355/isijinternational.42.1457
[11] Zhang, J. J., Wang, M. X., Yang, J., Liu, Q. X., Li, D. J.: Surface and Coatings Technology, *201*, 2007, p. 5186. doi:10.1016/j.surfcoat.2006.07.093
[12] Shah, H. N., Jayaganthan, R., Kaur, D., Chandra, R.: Thin Solid Films, *518*, 2010, p. 5762. doi:10.1016/j.tsf.2010.05.095
[13] Kong, Q., Ji, L., Hongxuan, L., Xiaohong, L., Youngjun, W., Chen, J., Zhou, H.: Applied Surface Science, *257*, 2011, p. 2269. doi:10.1016/j.apsusc.2010.09.086
[14] Forniés, E., Escobar Galindo, R., Sánchez, O., Albella, J. M.: Surface and Coatings Technology, *200*, 2006, p. 6047. doi:10.1016/j.surfcoat.2005.09.020
[15] Lin, J., Wu, Z. L., Zhang, X. H., Mishra, B., Moore, J. J., Sproul, W. D.: Thin Solid Films, *517*, 2009, p. 1887. doi:10.1016/j.tsf.2008.09.093
[16] Era, H., Ide, Y., Nino, A., Kishitake, K.: Surface and Coatings Technology, *194*, 2005, p. 265. doi:10.1016/j.surfcoat.2004.05.022
[17] Logothetidis, S., Patsalas, P., Sarakinos, K., Charitidis, C., Metaxa, C.: Surface and Coatings Technology, *180–181*, 2004, p. 637. doi:10.1016/j.surfcoat.2003.10.108
[18] Ehiasarian, A. P., Munz, W. D., Hultman, L., Helmersson, U., Petrov, I.: Surface and Coatings Technology, *163–164*, 2003, p. 267. doi:10.1016/S0257-8972(02)00479-6
[19] Lin, J., Sproul, W. D., Moore, J. J., Lee, S., Myers, S.: Surface and Coatings Technology, *205*, 2011, p. 3226. doi:10.1016/j.surfcoat.2010.11.039
[20] Hones, P., Sanjines, R., Lévy, F.: Surface and Coatings Technology, *94–95*, 1997, p. 398. doi:10.1016/S0257-8972(97)00443-X
[21] Odén, M., Almer, J., Hakansson, G., Olsson, M.: Thin Solid Films, *377–378*, 2000, p. 407. doi:10.1016/S0040-6090(00)01307-9
[22] Broszeit, E., Friedrich, C., Berg, G.: Surface and Coatings Technology, *115*, 1999, p. 9. doi:10.1016/S0257-8972(99)00021-3
[23] Lin, J., Moore, J. J., Sproul, W., Mishra, B., Wu, Z., Wang, J.: Surface and Coatings Technology, *204*, 2010, p. 2230. doi:10.1016/j.surfcoat.2009.12.013
[24] Zhang, G. A., Yan, P. X., Wang, P., Chen, Y. M., Zhang, J. Y.: Materials Science and Engineering A, *460–461*, 2007, p. 301. doi:10.1016/j.msea.2007.01.149
[25] Ortmann, S., Savan, A., Gerbig, Y., Haefke, H.: Wear, *254*, 2003, p. 1099. doi:10.1016/S0043-1648(03)00342-9
[26] Warcholinski, B., Gilewicz, A.: Journal of Achievements in Materials and Manufacturing Engineering, *37/2*, 2009, p. 498.
[27] Hudáková, M., Kusý, M., Sedlická, V., Grgač, P.: Materials and Technology, *41*, 2007, p. 81.
[28] Zhao, Z. B., Rek, Z. U., Yalisove, S. M., Bilello, J. C.: Surf. Coat. Techn., *185*, 2004, p. 329. doi:10.1016/j.surfcoat.2003.12.026
[29] Matthews, A., Leyland, A.: HTM, *56*, 2001, p. 5.
[30] Jurči, P., Dlouhý, I.: Appl. Surf. Sci, *257*, 2011, p. 10581. doi:10.1016/j.apsusc.2011.07.054
[31] Jurči, P., Hudáková, M.: Materials and Technology, *42*, 2008, p. 197.
[32] Hurkmans, T., Lewis, D. B., Brooks, J. S., Munz, W. D.: Surface and Coatings Technology, *86–87*, 1996, p. 192.